Pergamon

Tetrahedron 58 (2002) 3699–3708

TETRAHEDRON

Transformation of lactone to lactam in sarcophine and antimalarial activity of the resulting *N*-substituted azasarcophines

Khalid A. El Sayed,[a,*] Khaled Y. Orabi,[b] D. Chuck Dunbar,[c] Mark T. Hamann,[a,c] Mitchell A. Avery,[c,d] Yogesh A. Sabnis,[d] Jaber S. Mossa[b] and Farouk S. El-Feraly[b]

[a]*Department of Pharmacognosy, School of Pharmacy, The University of Mississippi, University, MS 38677, USA*
[b]*Department of Pharmacognosy, College of Pharmacy, King Saud University, Riyadh 11451 Saudi Arabia*
[c]*National Center for Natural Products Research, School of Pharmacy, The University of Mississippi, University, MS 38677, USA*
[d]*Department of Medicinal Chemistry, School of Pharmacy, The University of Mississippi, University, MS 38677, USA*

Received 30 January 2002; accepted 21 March 2002

Abstract—Sarcophine (**1**) is a furanocembranoid diterpene first reported from the Red Sea soft coral *Sarcophyton glaucum* with remarkable yields of up to 3% dry weight. Semisynthetic transformation of the lactone to lactam in sarcophine by reaction with benzyl and ethylamine afforded six new *N*-substituted azasarcophines (**2**–**7**), in addition to an asymmetric novel dimer **8**. The in vitro activity of azasarcophines against *Palsmodium falciparium* (D6 clone) and *P. falciparium* (W2 clone) are also discussed.

1. Introduction

Sarcophine is a furanocembranoid first reported by Kashman and co-workers in 1974 from the Red Sea soft coral *Sarcophyton glaucum*.[1] This compound exhibits a diverse range of bioactivities including anti-acetylcholine and competitive cholinesterase inhibitory activities on isolated guinea pig ileum,[2] noncompetitive reversible inhibition of rabbit skeletal muscle phosphofructokinase,[3] inhibition of Na^+, K^+-ATPase activity of rat brain,[4] anticancer,[5] and antidepressant activity in mice.[6] These interesting bioactivities initiated numerous attempts towards the total synthesis of sarcophine.[7–11] Sarcophine was also a target for several semisynthetic studies. Kashman and co-workers conducted acid-catalyzed transannular and reduction reactions on sarcophine to afford various epoxide opening and transannular reaction products.[12] Another study proposed the autoxidation of 16-deoxysarcophine to sarcophine, and rearranged peroxides and hydroxylated derivatives.[13] The use of selenium dioxide to oxidize sarcophine at C-13 and C-20 was also reported.[14] Herewith we report the transformation of lactone to lactam in sarcophine by reaction with benzyl and ethylamines and the in vitro antimalarial activity of these compounds against *Plasmodium falciparum*.

2. Results and discussion

An attempt to transform the lactone to lactam in sarcophine (**1**) to generate azasarcophines, in a similar fashion to those of artemisinin,[15] was conducted. Small scale reaction of **1** with several aqueous primary amines (R=methyl, ethyl, butyl, isobutyl, heptyl, 1-hydroxyethyl, and benzylamine) in toluene at room temperature showed positive results. Benzyl and ethylamine were selected for large scale reactions because of the chromatographic diversity of their products. Reaction of **1** with 30% aqueous benzylamine afforded the new products **2**–**4** (2.1, 1.8, and 2.2% yield, respectively). The same reaction using 30% aqueous ethylamine afforded the new products **5**–**8** (2.4, 1.6, 1.6, and 9.7% yield, respectively).

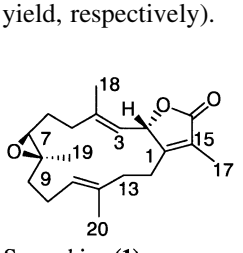

Sarcophine (**1**)

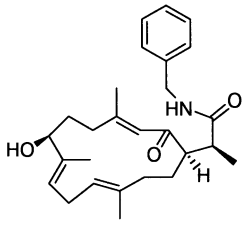

2

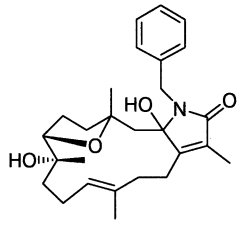

3

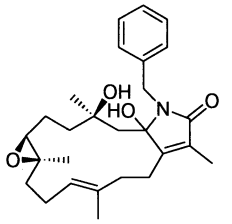

4

Keywords: sarcophine; antimalarial activity; *N*-substituted azasarcophines.
* Corresponding author. Present address: Department of Basic Pharmaceutical Sciences, College of Pharmacy, University of Louisiana at Monroe, 700 University Avenue, Monroe, LA 71209, USA. Tel.: +318-342-1725; fax: +318-342-3255; e-mail: pyelsayed@ulm.edu

0040–4020/02/$ - see front matter
PII: S0040-4020(02)00330-7

Table 1. ^{13}C and ^{1}H NMR data of compounds **2**–**4**

Position	**2**[a]		**3**		**4**	
	^{13}C[b]	^{1}H	^{13}C[b]	^{1}H	^{13}C[b]	^{1}H
1	54.3, d	2.65, ddd (10.8, 5.0, 5.0)	156.3, s	–	155.5, s	–
2	203.4, s	–	92.0, s	–	94.2, s	–
3	129.5, d	5.90, s	47.2, t	2.24, 2H, m	45.2, t	2.12, d (15.8); 2.00, d (15.8)
4	155.8, s	–	82.3, s	–	73.9, s	–
5	38.7, t	2.28, m; 2.01, ddd (17.1, 11.3, 4.0)	42.8, t	1.78, 2H, m	37.4, t	2.18, m; 1.68, m
6	29.7, t	1.94, m; 1.80, m	26.1, t	1.91, m; 1.87, m	24.5, t	2.17, m; 2.08, m
7	80.7, d	3.98, dd (10.3, 3.5)	83.6, d	3.97, dd (9.0, 6.4)	65.8, d	2.71, dd (9.0, 4.7)
8	135.7, s	–	73.5, s	–	59.5, s	–
9	126.9, d	5.31, dd (9.9, 5.5)	41.3, t	1.51, 2H, m	38.9, t	2.09, m; 1.18, m
10	27.6, t	2.86, m; 2.45, m	21.8, t	2.21, m; 2.00, m	24.7, t	2.28, m; 2.17, m
11	123.3, d	5.00, dd (8.3, 7.8)	127.1, d	5.68, dd (6.4, 6.2)	124.0, d	5.28, brd (6.4)
12	134.5, s	–	131.5, s	–	136.2, s	–
13	40.1, t	2.06, m; 1.95, m	33.4, t	2.46, m; 2.25, m	37.7, t	2.63, m; 2.33, m
14	28.9, t	1.98, m; 1.44, m	25.8, t	2.70, m; 2.61, m	25.0, t	2.80, m; 2.39, m
15	45.8, d	2.22, dq (9.8, 6.9)	126.2, s	–	128.1, s	–
16	175.0, s	–	171.5, s	–	170.9, s	–
17	16.8, q	1.03, 3H, d (6.9)	8.9, q	1.72, 3H, brs	8.4, q	1.79, 3H, brs
18	18.5, q	2.00, 3H, s	26.0, q	1.06, 3H, s	27.9, q	1.07, 3H, s
19	10.6, q	1.56, 3H, s	23.5, q	0.99, 3H, s	15.5, q	1.16, 3H, s
20	15.0, q	1.48, 3H, s	17.5, q	1.61, 3H, s	15.9, q	1.72, 3H, s
Benzyl						
1′	44.0, t	4.41, 2H, d (5.4)	44.6, t	4.91, d (15.3); 4.10, d (15.3)	42.5, t	4.68, d (15.6); 4.53, d (15.6)
2′	138.7, s	–	140.9, s	–	141.0, s	–
3′, 7′	128.2, d	7.25, 2H, brd (7.6)	129.4, d	7.39, 2H, brd (7.3)	129.3, d	7.45, 2H, d (7.5)
4′, 6′	129.1, d	7.30, 2H, dd (7.2, 7.2)	128.7, d	7.27, 2H,dd (7.4, 7.1)	129.0, d	7.29, 2H,dd (7.6, 7.5)
5′	127.9, d	7.31, d (7.2)	127.3, d	7.21, d (7.2)	127.6, d	7.23, d (7.6)
NH	–	5.91, brs	–	–	–	–
C-2OH	–	–	–	4.40, brs	–	6.15, brs
C-4OH	–	–	–	–	–	4.71, brs
C-7OH	–	NO	–	–	–	–
C-8OH	–	–	–	NO	–	–

In acetone d_6, 400 or 500 MHz for ^{1}H and 100 or 125 MHz for ^{13}C NMR. Coupling constants (J) are in Hz. NO=Not Observed.
[a] In $CDCl_3$.
[b] Carbon multiplicities were determined by DEPT135° experiments. s=quaternary, d=methine, t=methylene, q=methyl carbons.

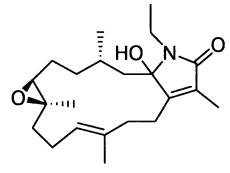

5

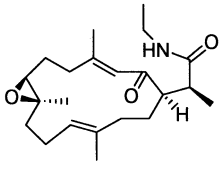

6

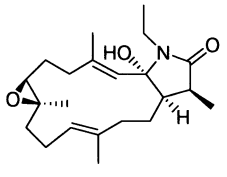

7

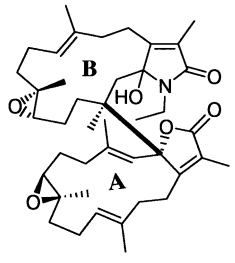

8

The HRFTMS spectrum of **2** displayed a molecular ion peak at m/z 446.2415 $[M+Na]^+$, suggesting the molecular formula $C_{27}H_{37}O_3N$ and ten degrees of unsaturation. The IR absorption bands at 1709 and 1658 cm^{-1} revealed the presence of ketone and amide carbonyl, respectively. The ^{1}H and ^{13}C NMR data of **2** (Table 1) indicated the opening of the butenolide and transformation of the lactone in **1** to an amide, and the formation of a ketone at C-2. Subsequently, a presumed E^1-like ammonium ion-catalyzed epoxide ring opening and elimination occur to, ultimately, lead to the formation of a $\Delta^{8,9}$ system. The ^{1}H NMR data of **2** (Table 1) show typical signals due to a benzyl functionality with five aromatic protons and a benzylic methylene doublet (H_2-1′, δ 4.41). H_2-1′ shows ^{3}J-HMBC correlation with the aromatic C-3′, C-7′ and with the carbonyl carbon C-16 (δ 175.0), confirming the transformation of the lactone to an amide. The methyl doublet at δ 1.03 was assigned C-17 based on its ^{3}J-HMBC correlation with C-16 amide carbonyl and C-1. The ketone resonance at δ 203.4 was assigned C-2 as suggested from its HMBC correlations with the olefinic H-3 and H_2-14. This ketone carbon is shifted upfield due to the α,β-unsaturation at C-3/C-4. The doublet of doublets at δ 3.98 was assigned as H-7 as indicated from the ^{3}J-HMBC correlation with C-19. The latter methyl proton singlet also showed HMBC correlations with C-8 (δ 135.7) and C-9 (δ 126.9) which confirmed the $\Delta^{8,9}$ system. The relative stereochemistry of **2** was established by analysis of NOESY data, molecular modeling (Fig. 1), and comparison of ^{13}C NMR data with those of known compounds.[5,16,17] The proton H-1 was assigned to be α-oriented based on the similarity of $J_{1/14a}$ and $J_{1/14b}$ values (5.0 Hz each) with those of singardin, sinuleptolide and 5-*epi*-sinuleptolide.[16] The α-orientation of H-5a at δ 2.01 was deduced by matching its J values with those previously reported for 5β-hydroxysarcophine.[5]

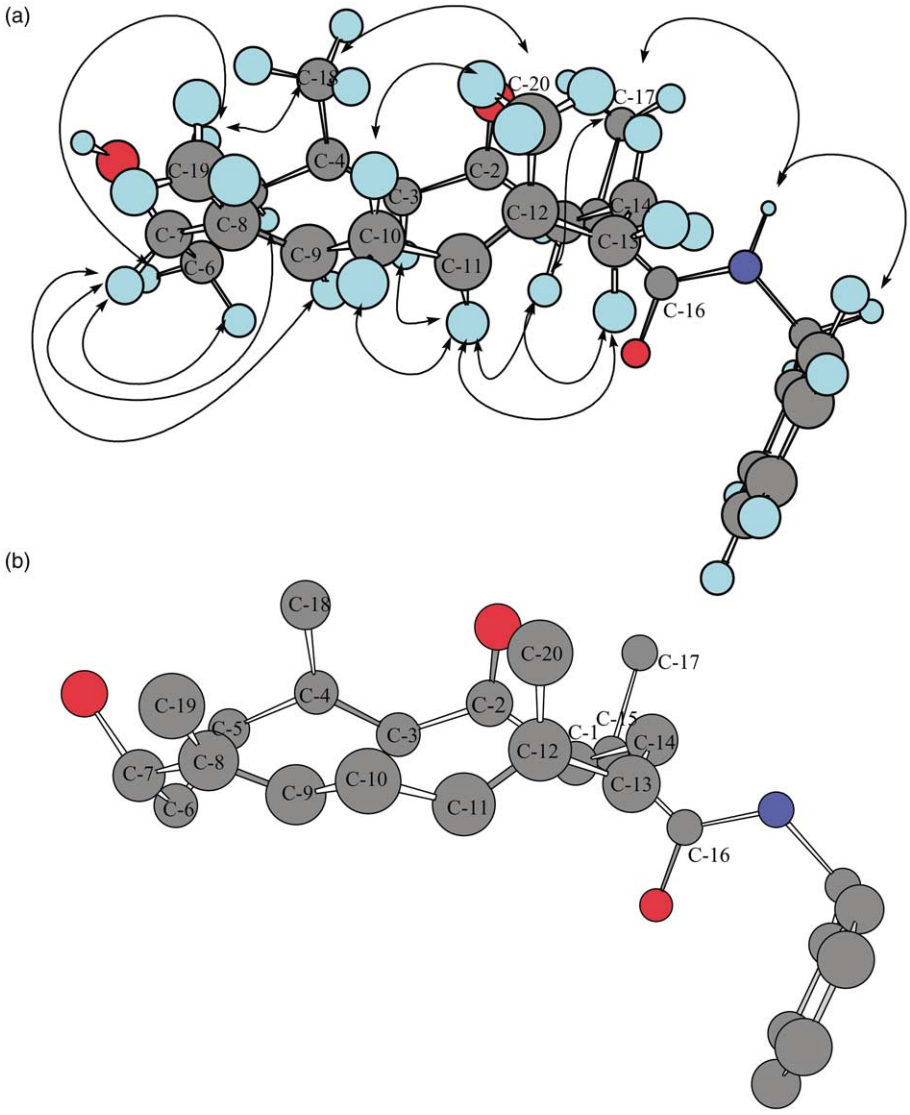

Figure 1. The lowest energy conformation for **2**, shown in (a) as a Chem3D file, but calculated by molecular dynamics and simulated annealing in Sybyl v6.5 (Tripos Associates). Arrows indicate key NOESY correlations. The identical structure for **2a** is shown in (b) in which the H's, and NOESY arrows are omitted for clarity.

Likewise, H-7 was assigned to be α-oriented as it showed NOESY correlation with the α-oriented H-5a (Fig. 1). The α-oriented H-6 at δ 1.80, based on its NOESY correlation with H-5a, also shows NOESY correlation with H-7 (Fig. 1). This is further confirmed by comparing the downfield shift of C-7 in **2** (+2.9 ppm) with that of the closely related (7*R*,14*S*,1*E*,3*E*,8*E*,11*E*)-cembra-1,3,8,11-tetraene-7,14-diol, indicating opposite configuration.[17] The absolute stereochemistry of C-7 in the latter cembranoid was established using Mosher esters.[17] Fig. 1 represents the Chem3D structure of the lowest energy conformation of **2** calculated by molecular dynamics and simulated annealing in SYBYL (Tripos Asso. Inc., St. Louis, MO) version 6.7. Analysis of NOESY data further supported this conformation. Fig. 1 indicates that the presence of $\Delta^{8,9}$ system encourage the existence of the C-6–C-10 segment in a half-chair conformer and forces the methine C-7 and the methylene C-10 to be in an anti-configuration. Fig. 1 indicates that H-1 and C-17 methyl group are *trans* to each others, with a dihedral angle of 177.6°. Fig. 1 also shows the gauche confirmation of H-1 and H-15, explaining the large $J_{1/15}$ value (10.8 Hz). Molecular modeling calculations indicated that if the methyl C-17 is β-oriented, the distance between H-1 and H-15 will be 2.465 Å, while if C-17 methyl is α-oriented, the distance H-1–H-15 will equal to 3.049 Å. This is further supported by the NOESY correlation between H-1 and H-15 and C-17 methyl group, which then should be β in disposition (Fig. 1).

The HRFTMS spectrum of **3** displayed a molecular ion peak at *m/z* 440.2799 $[M+H]^+$, suggesting the molecular formula $C_{27}H_{37}O_4N$ and ten degrees of unsaturation. The IR absorption band at 1683 cm^{-1} indicated a lactam carbonyl. The ^1H and ^{13}C NMR data of **3** (Table 1) indicated the transformation of the lactone to a lactam functionality, and the aqueous-mediated ring opening of the oxirane moiety with the formation of a 4,7-oxatransannular product. The quaternary carbon at δ 92.0 was assigned to be C-2 based on its ^3J-HMBC correlation with the benzylic methylene protons (H_2-1′) and ^2J-HMBC correlation with H_2-3. The

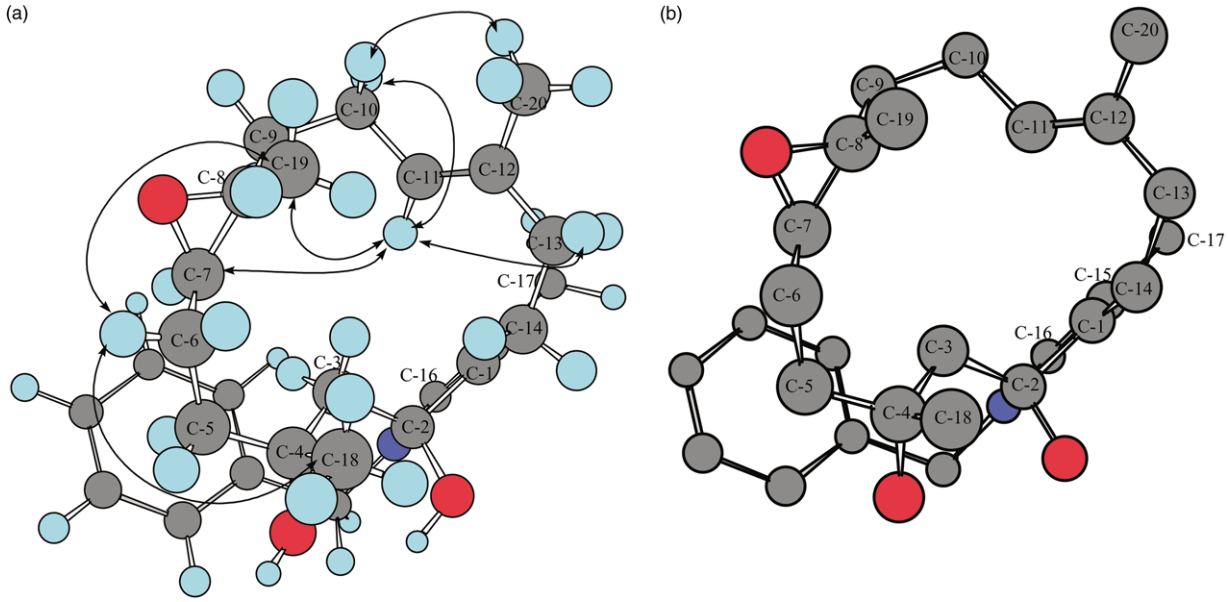

Figure 2. The lowest energy conformation for **4**, shown in (a) as a Chem3D file, but calculated by molecular dynamics and simulated annealing in Sybyl v6.5 (Tripos Associates). Arrows indicate key NOESY correlations. The identical structure for **4a** is shown in (b) in which the H's, and NOESY arrows are omitted for clarity.

exchangeable broad singlet at δ 4.40 shows ^{2}J-HMBC correlation with C-2 and ^{3}J-HMBC correlation with C-1 and C-3. The quaternary oxygenated carbon at δ 82.3 was assigned to be C-4 based on its ^{2}J-HMBC correlation with H_3-18, H_2-3, and H_2-5, in addition to ^{3}J-HMBC correlation with H_2-6. The downfield oxygenated methine at δ 3.97 was assigned to be H-7 as indicated from its ^{3}J-HMBC correlation with H_2-5, H_2-9, and H_3-19. Proton H-7 also shows COSY coupling with H_2-6 which in turn is COSY-coupled to H_2-5. The assignment of C-5 is well established through its ^{3}J-HMBC correlation with H_3-18 and H_2-3. The assignment of C-8 was primarily based on its ^{3}J-HMBC correlation with H_2-6 as well as ^{2}J-HMBC correlation with H-7 and H_3-19. The relative stereochemistry around the chiral center C-2 is ambiguous in the hemiaminal product **3**. The proton H-7 was assigned α-oriented since the splitting

Table 2. ^{13}C and ^{1}H NMR data of compounds **5**–**7**

Position	**5**		**6**		**7**	
	$^{13}C^{a}$	^{1}H	$^{13}C^{a}$	^{1}H	$^{13}C^{a}$	^{1}H
1	153.6, s	–	52.9, d	2.71, m	50.1, d	1.80, m
2	93.1, s	–	205.3, s	–	92.0, s	–
3	41.0, t	2.12, m; 1.87, m	128.6, d	6.15, s	130.0, d	5.36, brs
4	27.8, d	1.53, m	154.8, s	–	137.0, s	–
5	31.5, t	2.27, m; 1.33, m	37.9, t	2.36, m;; 2.26, m	37.0, t	1.83, m; 1.40, m
6	24.3, t	2.09, m;; 1.40, m	22.4, t	1.54, 2H, m	27.0, t	1.87, m; 1.70, m
7	66.5, d	2.18, brd (8.2)	61.1, d	2.88, brs	60.1, d	2.83, brs
8	61.3, s	–	60.4, s	–	59.2, s	–
9	38.9, t	2.13, m; 0.99, m	25.3, t	1.80, 2H, m	36.9, t	2.28, m; 2.12, m
10	24.6, t	2.30, m;; 2.11, m	37.0, t	2.25, m; 2.01, m	22.6, t	2.00, m; 1.92, m
11	124.2, d	5.10, dd (7.2, 7.0)	126.0, d	4.77, brs	126.0, d	5.06, dd (6.2, 5.4)
12	134.3, s	–	134.8, s	–	133.9, s	–
13	35.9, t	2.31, 2H, m	36.9, t	2.36, m; 2.26, m	36.1, t	2.29, m; 2.06, m
14	22.8, t	2.64, m; 2.52, m	28.8, t	1.72, m; 1.52, m	26.0, t	1.89, m; 1.53, m
15	130.6, s	–	45.0, d	2.24, m	41.7, d	2.07, m
16	175.2, s	–	174.8, s	–	175.7, s	–
17	9.4, q	1.78, 3H, brs	16.6, q	1.07, 3H, d (6.5)	15.4, q	1.13, 3H, d (7.0)
18	20.4, q	0.87, 3H, d (6.6)	18.1, q	2.01, 3H, s	15.8, q	1.74, 3H, brs
19	16.6, q	1.23, 3H, s	18.9, q	1.18, 3H, s	17.5, q	1.30, 3H, s
20	16.4, q	1.71, 3H, s	14.9, q	1.43, 3H, s	15.3, q	1.55, 3H, s
Ethyl						
1′	34.2, t	3.61, m; 3.11, m	34.4, t	3.36, m; 3.18, m	35.0, t	3.38, m; 3.10, m
2′	15.3, q	1.23, 3H, t (6.2)	14.6, q	1.00, 3H, t (6.2)	14.4, q	1.11, 3H, t (6.8)
NH	–	–	–	6.27, brd (3.6)	–	–
C-2OH	–	NO	–	–	–	4.70, s

In $CDCl_3$, 400 MHz for ^{1}H and 100 MHz for ^{13}C NMR. Coupling constants (J) are in Hz. NO=Not Observed.
[a] Carbon multiplicities were determined by DEPT135° experiments. s=quaternary, d=methine, t=methylene, q=methyl carbons.

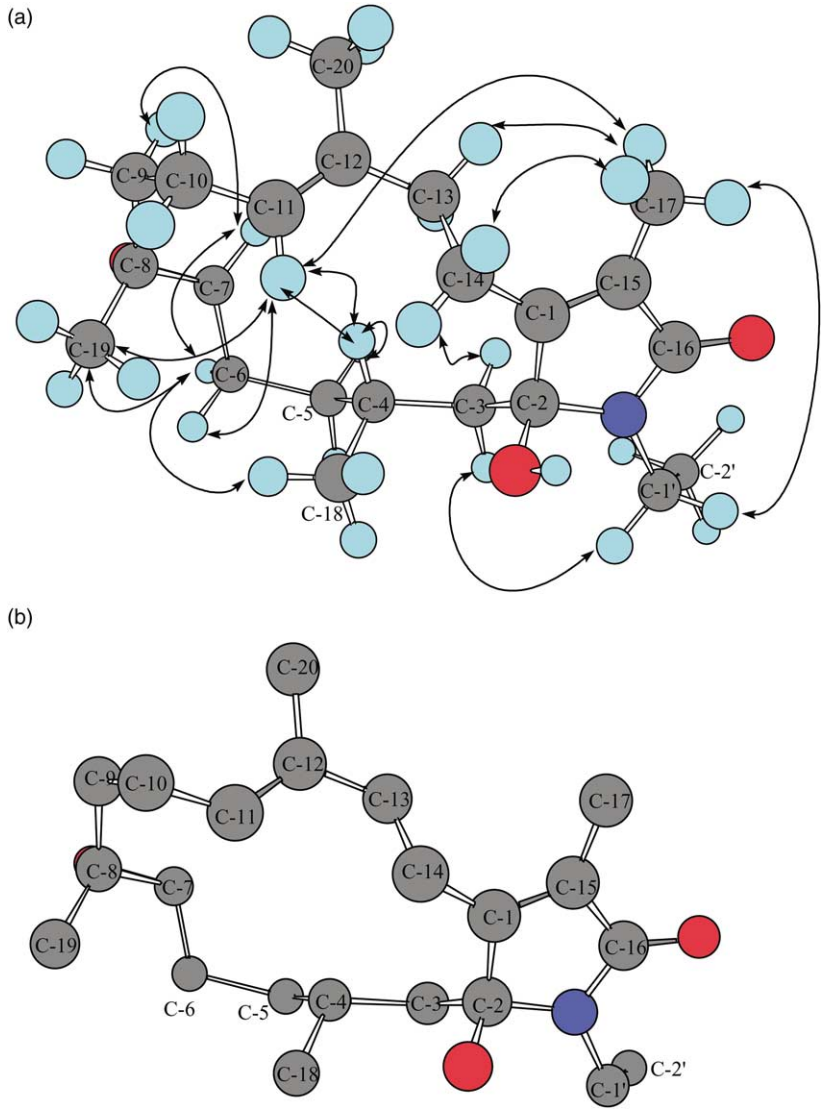

Figure 3. The lowest energy conformation for **5**, shown in (a) as a Chem3D file, but calculated by molecular dynamics and simulated annealing in Sybyl v6.5 (Tripos Associates). Arrows indicate key NOESY correlations. The identical structure for **5a** is shown in (b) in which the H's, and NOESY arrows are omitted for clarity.

pattern and *J* (dd, 9.0, 6.4 Hz) were similar to those reported for H-7 in 7β,8α-dihydroxydeepoxysarcophine (dd, *J*=9.6, 9.5 Hz).[5] The β-oriented H-7 was reported as a doublet in 7α,8β-dihydroxydeepoxysarcophine (*J*=13.5 Hz), for which the structure was proved by X-ray-crystallography,[5] and in 7,12-oxa-$\Delta^{8,9}$ deepoxysarcophine (*J*=13.5 Hz), which is a related transannular tetrahydrooxepine generated from sarcophine by $SnCl_4$/ethanol/−60°.[12] The opening of the 7,8-epoxide is expected to occur with inversion of configuration and hence the hydroxy group at C-8 should be *trans* to the β-oriented C-7 oxygen functionality. There were not enough NOESY data to establish the stereochemistry around C-4 which can be left ambiguous. However, based on the required 5-*exo*-tet ring cyclization, it seems likely that C-4 is in the *R* configuration.

The HRFTMS spectrum of **4** displayed a molecular ion peak at *m/z* 440.2610 $[M+H]^+$, suggesting the molecular formula $C_{27}H_{37}O_4N$ and ten degrees of unsaturation. The ^1H and ^{13}C NMR data of **4** (Table 1) suggested a close similarity to **3** with an intact oxirane group. The quaternary carbon at δ 73.9 was assigned to be C-4 as indicated from the ^2J-HMBC correlation with H_3-18, H_2-3, and H_2-5. The exchangeable singlet at δ 4.71 displayed ^2J-HMBC correlation to C-4, confirming hydroxylation at C-4. The medium NOESY correlation (Fig. 2) between H_3-19 and H-6b (δ 2.08) suggested the α-orientation of H-6b, which in turn shows medium NOESY correlation to H_3-18. Again, molecular modeling calculations further supported this assumption. The calculated distance between H-6b and C-19 methyl is 2.806 Å while the distance between H6b and the methyl C-18 is 2.889 Å. On the other hand, the calculated distances between H6a and C-19 and C-18 methyl groups were found to be 3.835 and 4.122 Å, respectively.

The HRFTMS spectrum of **5** displayed a molecular ion peak at *m/z* 362.2755 $[M+H]^+$, suggesting the molecular formula $C_{22}H_{35}O_3N$ and six degrees of unsaturation. The IR absorption band at 1679 cm^{-1} indicated a lactam carbonyl. The ^1H and ^{13}C NMR data of **5** (Table 2) indicated the formation of

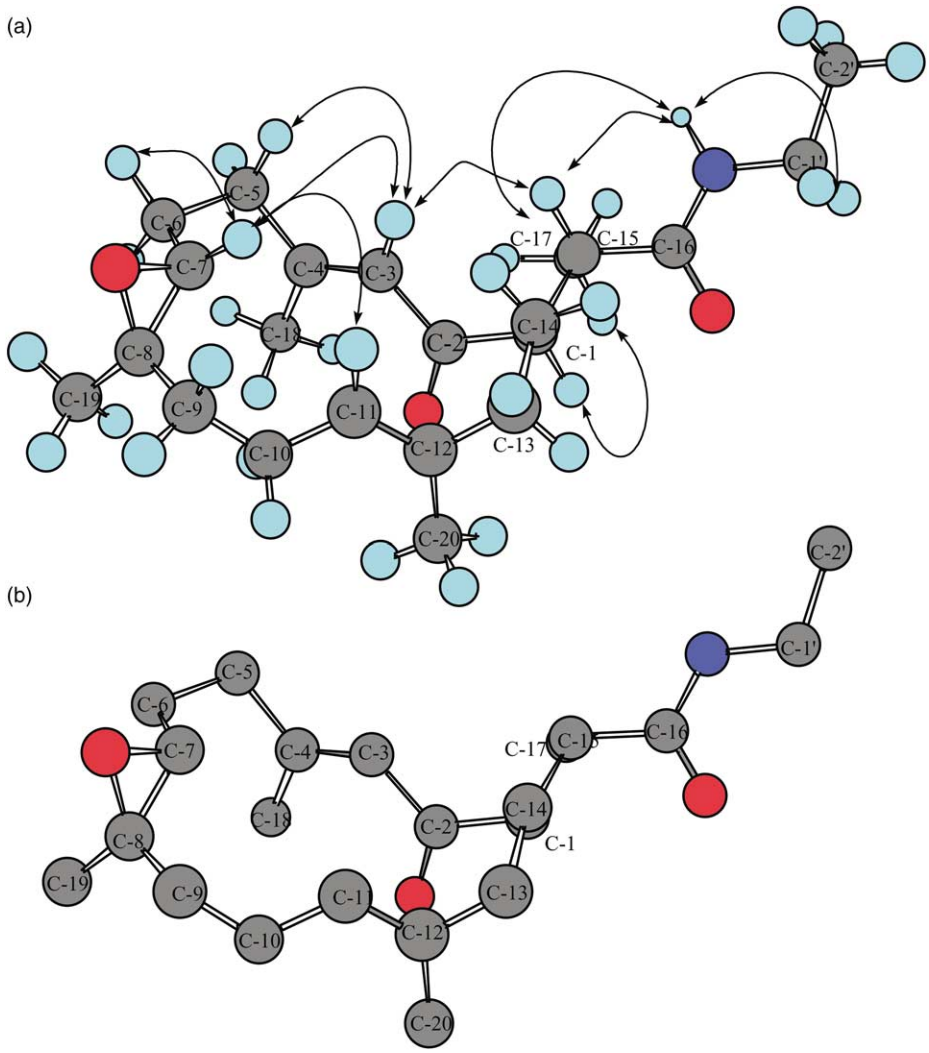

Figure 4. The lowest energy conformation for **6**, shown in (a) as a Chem3D file, but calculated by molecular dynamics and simulated annealing in Sybyl v6.5 (Tripos Associates). Arrows indicate key NOESY correlations. The identical structure for **6a** is shown in (b) in which the H's, and NOESY arrows are omitted for clarity.

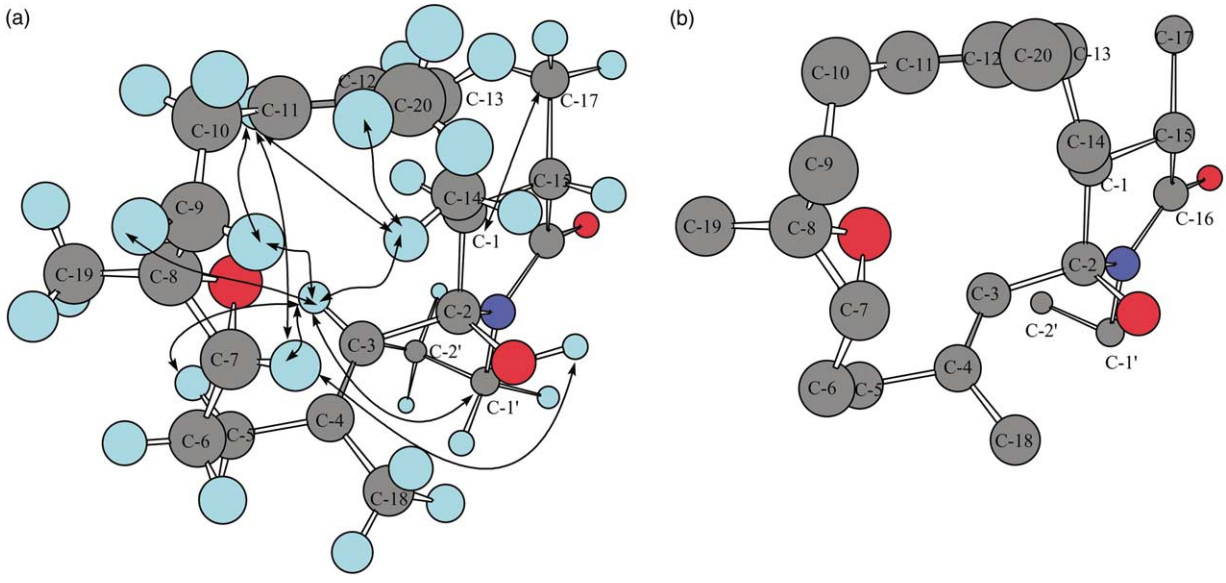

Figure 5. The lowest energy conformation for **7**, shown in (a) as a Chem3D file, but calculated by molecular dynamics and simulated annealing in Sybyl v6.5 (Tripos Associates). Arrows indicate key NOESY correlations. The identical structure for **7a** is shown in (b) in which the H's, and NOESY arrows are omitted for clarity.

Table 3. ^{13}C and ^{1}H NMR data of compounds **8**

Position	**8**				
	Monomer A		Position	Monomer B	
	$^{13}C^{a}$	^{1}H		$^{13}C^{a}$	^{1}H
1	164.8, s	–	1′	154.4, s	–
2	93.7, s	–	2′	92.4, s	–
3	118.1, d	5.59, s	3′	37.1, t	1.81, m; 1.73, m
4	140.4, s	–	4′	43.8, s	–
5	38.5, t	2.21, m; 2.02, m	5′	29.9, t	1.78, 2H, m
6	24.5, t	2.07, m; 1.70, m	6′	29.2, t	2.10, 2H, m
7	62.4, d	2.69, m	7′	65.2, d	2.65, m
8	60.2, s	–	8′	59.8, s	–
9	39.4, t	2.20, m; 2.02, m	9′	37.0, t	2.11, m; 2.01, m
10	24.7, t	2.11, m; 1.80, m	10′	23.4, t	2.40, m; 2.30, m
11	125.0, d	5.02, dd (8.0, 6.4)	11′	121.9, d	5.18, brs
12	134.4, s	–	12′	136.2, s	–
13	38.0, t	2.20, m; 2.02, m	13′	35.4, t	2.47, m; 2.25, m
14	25.9, t	2.77, m; 2.30, m	14′	23.7, t	2.30, m; 2.21, m
15	125.7, s	–	15′	128.8, s	–
16	174.4, s	–	16′	170.8, s	–
17	10.0, q	1.90, 3H, s	17′	9.1, q	1.77, 3H, brs
18	17.1, q	1.53, 3H, s	18′	18.6, q	0.93, 3H, s
19	16.5, q	1.22, 3H, s	19′	15.7, q	1.10, 3H, s
20	14.9, q	1.58, 3H, s	20′	17.3, q	1.63, 3H, s
			Ethyl		
	–	–	1″	34.9, t	3.53, m; 2.93, m
	–	–	2″	15.3, q	1.19, 3H, t (6.8)

In $CDCl_3$, 400 MHz for ^{1}H and 100 MHz for ^{13}C NMR. Coupling constants (J) are in Hz.
[a] Carbon multiplicities were determined by DEPT135° experiments. s=quaternary, d=methine, t=methylene, q=methyl carbons.

an *N*-ethylazasarcophine derivative. The methyl triplet at δ 1.23 is assigned as the terminal H_3-2′ of ethylamine as suggested from its HMBC and COSY coupling to the downfield nitrogenated methylene protons H_2-1′. The latter methylene displayed ^{3}J-HMBC correlation to the downfield quaternary carbon at δ 93.1 (C-2) and the amide carbonyl (δ 175.2, C-16). The methyl doublet at δ 0.87 is assigned H_3-18 as indicated from its ^{3}J-HMBC correlation to C-3 and C-5, in addition to ^{2}J-HMBC correlation to C-4. The α-orientation of H_3-18 was suggested from its weak NOESY correlation (Fig. 3) to H-6b (δ 1.40) which in turn shows medium NOESY correlation to the α-oriented methyl H_3-19. Molecular modleing calculations supported this assignment. The calculated distance between H-6b and C-19 methyl is 2.745 Å while the distance between H6b and the methyl C-18 is 2.955 Å. On the other hand, the calculated distances between H6a and C-19 and C-18 methyl groups were found to be 3.871 and 4.185 Å, respectively.

The HRFTMS spectrum of **6** displayed a molecular ion peak at *m/z* 362.2682 $[M+H]^+$, suggesting the molecular formula $C_{22}H_{35}O_3N$ and six degrees of unsaturation. The IR absorption bands at 1708 and 1677 cm^{-1} indicated a ketone and an amide carbonyl. The ^{1}H and ^{13}C NMR data of **6** (Table 2) indicated the formation of an *N*-ethylazasarcophine derivative with an open butenolide moiety and C-2 ketone. The methylene protons at δ 3.36 and 3.18 were assigned H_2-1′. These protons display COSY coupling to the H_3-2′ methyl triplet at δ 1.00 and the exchangeable broad doublet at δ 6.27 (NH). Both H_2-1′ and the methyl doublet H_3-17 show ^{3}J-HMBC correlation to the amide carbonyl C-16 (δ 174.8), confirming the opened butenolide side chain. The stereochemistry around C-1 and C-15 was proven in a way similar to that used in **2** (Fig. 4).[5,16]

The HRFTMS spectrum of **7** displayed a molecular ion peak at *m/z* 362.2792 $[M+H]^+$, suggesting the molecular formula for $C_{22}H_{35}O_3N$ and six degrees of unsaturation. The IR, ^{1}H and ^{13}C NMR data of **7** (Table 2) indicated close similarity to **5** with $\Delta^{3,4}$ instead of $\Delta^{1,15}$. The olefinic methine carbon at δ 130.0 was assigned C-3 as suggested by the ^{3}J-HMBC correlation with H-1, H_3-18 and the exchangeable proton singlet at δ 4.70 (C-2 hydroxy). Fig. 5 represents the Chem3D structure of the lowest energy conformation of **7**, calculated by molecular dynamics and simulated annealing in Sybyl v6.5. The NOESY correlation between the C-2 hydroxy group and α-H-7 suggested similar orientation. The stereochemistry around C-1 and C-15 was similar to those of **2**. As in sarcophine, the C7/C8 oxirane functionality forced the segment C-5–C-8 to be in a half-chair conformer and hence the methine C-6 and the methylene C-9 to be in an anti-configuration. This is supported by the NOESY correlation of H_2-9 with the olefinic H-3 and H-11.

The HRFTMS spectrum of **8** displayed a molecular ion peak at *m/z* 676.4512 $[M+H]^+$, suggesting the molecular formula $C_{42}H_{61}O_6N$ and thirteen degrees of unsaturation. The IR absorption bands at 1748 and 1677 cm^{-1} indicated lactone and lactam carbonyls. The ^{1}H and ^{13}C NMR data of **8** (Table 3) indicated an asymmetric carbon–carbon dimerization with an intact sarcophine molecule as monomer A and monomer B which is an *N*-ethylazasarcophine derivative, similar to **5**. The methyl singlet at δ 0.93 is assigned H_3-18′. This was based on its ^{3}J-HMBC correlation with C-3′ and C-5′ as well as ^{2}J-HMBC correlation with C-4′. The ^{3}J-HMBC correlation between H_3-18′ in monomer B and C-2 in monomer A confirmed the C–C connection between both monomers. The stereochemistry of the connection C-2/C-4′ was assigned as β-oriented since the

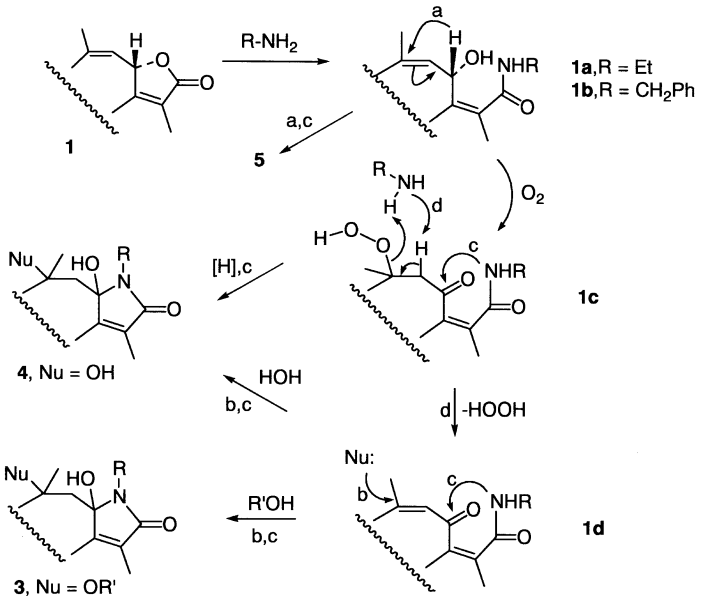

Scheme 1. Plausible mechanism of formation of compounds **3**–**5**. Key: (a) 1,3-sigmatropic shift; (b) nucleophilic 1,4-addition; (c) aminol ring formation; (d) retro-1,4-addition.

C-2 lactone in monomer A must retain the original α-orientation of the parent compound **1**. The NOESY correlation between H_3-17 and H_3-17′ suggested the location of the monomer A lactone and monomer B lactam on the same side.

A plausible mechanism of reaction of sarcophine with amines is proposed in Schemes 1 and 2. As shown in Scheme 1, the lactone is opened leading to amide formation and a free C-2α hydroxy group (**1a** and **1b**). Migration of $\Delta^{3,4}$ to C-2/C-3 provides **5** by an apparent 1,3-sigmatropic shift. Alternatively, hydride might be delivered to **1d** by path b where the Nu is a **1a** or **1b** C-2 methine proton. Hydroperoxidation of **1a** or **1b** via an ene-type process could lead to the hydroperoxide **1c**, from which loss of hydrogen peroxide by a retro-Michael process should furnish **1d**. With highly reactive **1d** in place, additions of alcohols or water leads, after ring closure, to products **3** and **4**. In Scheme 2, migration of $\Delta^{1,15}$ to C-15/C-16 with $\Delta^{1,2}$ formation would give the dienol intermediate with two free hydroxy groups at C-2 and C-16, tautomerization would then lead to the C-2/C-16 dicarbonyls **2** and **6**. Additionally, subsequent cyclization of nitrogen at C-2 by pathway a leads to compound **7**. Finally, the interesting dimer **8** probably arises via the furanoid enol of **1** undergoing conjugate-addition to an unidentified intermediate dienone, i.e., $\Delta^{1,15}$-dehydro-**6**.

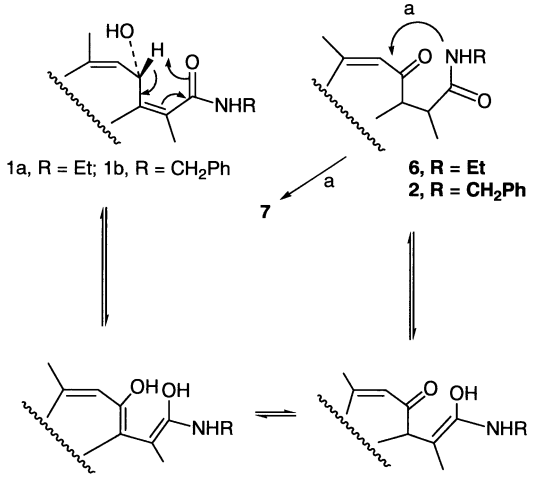

Scheme 2. Plausible mechanism of formation of compounds **2**, **6**, and **7**. Key: (a) aminol ring formation.

All azasarcophines were tested for cytotoxicity and in vitro antimalarial activity to check the effect of the amide functionality since sarcophine is not active in either assays. All compounds **2**–**8** did not show significant cytotoxicity against P-388, A-549, MEL-28, and HT-29 cells. Of all tested compounds, **2**, **3**, and **8** display in vitro antimalarial activity against *Palsmodium falciparium* (D6 clone)[18] with IC_{50} <529, 2800, and 1800 ng/mL, with selectivity indices >9.0, >1.7, and >2.6, respectively. These compounds were less active against *P. falciparium* (W2 clone) with IC_{50} 3200, 4100, and 2200 ng/mL, with selectivity indices >1.5, >1.2, and >2.2, respectively. Chloroquine and artemisinin were used as standard references and they show IC_{50} of 16 and 13 ng/mL, respectively, against *P. falciparum* (D6 clone) and IC_{50} of 165 and 6 ng/mL, respectively, against *P. falciparum* (W2 clone). The possibility of using other substituted amines to generate new analogues bodes well for enhancement of antimalarial activity.

3. Experimental

3.1. General experimental procedure

Melting points are uncorrected. The ^1H and ^{13}C NMR spectra were recorded in $CDCl_3$, on NMR spectrometers operating at 400 or 500 MHz for ^1H, and 100 or 125 MHz for ^{13}C NMR. The HRMS spectra were measured using a Bioapex FTMS with electrospray ionization. TLC analyses were carried out on precoated silica gel G_{254} 500 μm, with

the following developing system: $CHCl_3$–MeOH (95:5) or (94:6). For column chromatography, Si gel 60, 40 μm was used.

3.2. Computational methods

All computer aided molecular modeling was performed on a Silicon Graphics Octane2 workstation with dual R12000 processors. The diastereomeric forms of the compounds (**2**–**7**) were drawn and placed into databases using SYBYL v6.7 (Tripos Asso. Inc., St. Louis, MO). Prior to performing conformational searches on the databases, the diastereomers were first minimized employing a Tripos Force Field using the conjugate gradient method with a cutoff value of 0.05 kcal/mol and Gasteiger–Hückel charges. A distance-dependent dielectric constant of 0.78 was used to simulate the environment in which NOESY determinations were conducted, deuterochloroform. The databases were subjected to a molecular dynamics (MD) calculation, performed at constant temperature which corresponded to the NVT ensemble. Exploration of the conformational space was achieved by simulating the motions at 2000 K and then slowly cooling to 50 K. A time step of 1 fs (10^{-15}), a long non-bonding cutoff distance of 12 Å, and a distance dependent dielectric of $\varepsilon=4$ were used. The conformations generated by the dynamics run were further subjected to simulated annealing (SA). No restraints were applied during annealing as the lowest energy diastereomer in all the molecules was to be determined. Hence, all the possible diastereomers for the molecules (**2**–**7**) were subjected to MD-SA. The annealing process involved heating the system to 700 K for 500 fs and gradually annealing it to 200 K for 1000 fs, for a total of 10 cycles. This insured that several different low energy conformations of each molecule were obtained. The generated conformations were further minimized employing the same minimization technique described above. This eventually helped to obtain the lowest energy conformation in each of the databases (diastereomers).

3.3. Reaction of benzylamine with 1

A solution of 247 mg of **1** in 4 mL toluene was added to 1.1 mL 30% aqueous benzylamine. The reaction mixture was stirred for 120 h at room temperature. A brine solution (10 mL) was then added and the solution was extracted with $CHCl_3$ (2×10 mL). The organic layer was washed with H_2O (2×10 mL), dried over anhydrous Na_2SO_4 and evaporated under reduced pressure. The residue (520 mg) was fractionated on Si gel 60 (50 g) using cyclohexane–EtOAc, gradient elution, followed by CPTLC on Si gel G_{254}, using $CHCl_3$–MeOH (98:2) to afford **2** (5.1 mg, R_f 0.80, $CHCl_3$–MeOH 95:5), **3** (4.5 mg, R_f 0.52, $CHCl_3$–MeOH 95:5) and **4** (5.4 mg, R_f 0.42, $CHCl_3$–MeOH 95:5).

3.4. Reaction of ethylamine with 1

A solution of 289 mg of **1** in 4 mL toluene was added to 1.1 mL 30% aqueous ethylamine. The reaction mixture was stirred for 56 h at room temperature and worked up as the previous reaction. The residue (567 mg) was fractionated by MPLC on Si gel 60 (50 g) using $CHCl_3$–MeOH, gradient elution, followed by repeated CPTLC on Si gel G_{254}, using $CHCl_3$–MeOH (98:3) to afford **5** (6.9 mg, R_f 0.21, $CHCl_3$–MeOH 94:6), **6** (4.6 mg, R_f 0.37, $CHCl_3$–MeOH 94:6), **7** (4.6 mg, R_f 0.51, $CHCl_3$–MeOH 94:6), and **8** (28.0 mg, R_f 0.36, $CHCl_3$–MeOH 95:5).

3.4.1. Compound (2). Colorless oil, $[\alpha]_D^{25}=+7.0°$ (*c* 0.70, $CHCl_3$); UV λ_{max} (log ε) (MeOH) 244 (3.68), 238 (3.64), 221 (3.61) nm; IR ν_{max} (neat) 3324, 2954–2856, 1709, 1658, 1613, 1549, 1454, 1377, 758 cm^{-1}; ^1H and ^{13}C NMR, see Table 1. HRFTMS *m/z* calculated for $C_{27}H_{37}O_3NNa$ $(M+Na)^+$ 446.2671, found 446.2415.

3.4.2. Compound (3). Colorless oil, $[\alpha]_D^{25}=-22.0°$ (*c* 0.70, $CHCl_3$); UV λ_{max} (log ε) (MeOH) 250 (3.53), 231 (3.52), 223 (3.49) nm; IR ν_{max} (neat) 3340, 2954–2853, 1683, 1613, 1454, 1136, 758 cm^{-1}; ^1H and ^{13}C NMR, see Table 1. HRFTMS *m/z* calculated for $C_{27}H_{38}O_4N$ $(M+H)^+$ 440.2800, found 440.2799.

3.4.3. Compound (4). Colorless oil, $[\alpha]_D^{25}=-41.0°$ (*c* 0.70, $CHCl_3$); UV λ_{max} (log ε) (MeOH) 256 (3.52), 244 (3.58), 238 (3.60) nm; IR ν_{max} (neat) 3340, 2923–2876, 1675, 1613, 1441, 1054, 751 cm^{-1}; ^1H and ^{13}C NMR, see Table 1. HRFTMS *m/z* calculated for $C_{27}H_{38}O_4N$ $(M+H)^+$ 440.2800, found 440.2610.

3.4.4. Compound (5). Colorless oil, $[\alpha]_D^{25}=-9.0°$ (*c* 0.70, $CHCl_3$); UV λ_{max} (log ε) (MeOH) 261 (3.31), 246 (3.35), 241 (3.36), 226 (3.30) nm; IR ν_{max} (neat) 3341, 2954–2857, 1679, 1454, 1382, 1046, 754 cm^{-1}; ^1H and ^{13}C NMR, see Table 2. HRFTMS *m/z* calculated for $C_{22}H_{36}O_3N$ $(M+H)^+$ 362.2695, found 362.2755.

3.4.5. Compound (6). Colorless oil, $[\alpha]_D^{25}=+15.0°$ (*c* 0.70, $CHCl_3$); UV λ_{max} (log ε) (MeOH) 244 (3.69), 224 (3.68) nm; IR ν_{max} (neat) 3355, 2971–2877, 1708, 1677, 1550, 1453, 1378, 1086, 753 cm^{-1}; ^1H and ^{13}C NMR, see Table 2. HRFTMS *m/z* calculated for $C_{22}H_{36}O_3N$ $(M+H)^+$ 362.2695, found 362.2682.

3.4.6. Compound (7). Colorless oil, $[\alpha]_D^{25}=+30.0°$ (*c* 0.70, $CHCl_3$); UV λ_{max} (log ε) (MeOH) 254 (3.70), 234 (3.70), 230 (3.71) nm; IR ν_{max} (neat) 3371, 2955–2857, 1664, 1495, 1427, 1381, 1071 cm^{-1}; ^1H and ^{13}C NMR, see Table 2. HRFTMS *m/z* calculated for $C_{22}H_{36}O_3N$ $(M+H)^+$ 362.2695, found 362.2792.

3.4.7. Compound (8). Colorless oil, $[\alpha]_D^{25}=-4.0°$ (*c* 0.70, $CHCl_3$); UV λ_{max} (log ε) (MeOH) 253 (3.16), 249 (3.17), 244 (3.17), 239 (3.16), 224 (3.12) nm; IR ν_{max} (neat) 3371, 2982–2875, 1748, 1677, 1453, 1383, 1215, 1061, 761 cm^{-1}; ^1H and ^{13}C NMR, see Table 3. HRFTMS *m/z* calculated for $C_{42}H_{62}O_6N$ $(M+H)^+$ 676.4577, found 676.4512.

Acknowledgements

John Trott, University of Mississippi, is acknowledged for performing antimalarial assay. This work was supported in part by a Cooperative Agreement with the Center for Disease Control UR3/CCU418652 (MAA) and the College of Pharmacy Research Center, King Saud University, grant number CPRC 65. BIOMAR, S. A. is acknowledged for conducting the cytotoxicity assays.

References

1. Bernstein, J.; Shmeuli, U.; Zadock, E.; Kashman, Y.; Neeman, I. *Tetrahedron* **1974**, *30*, 2817–2824.
2. Neeman, I.; Fishelson, L.; Kashman, Y. *Toxicon* **1974**, *12*, 593–598.
3. Erman, A.; Neeman, I. *Toxicon* **1977**, *15*, 207–215.
4. Suleimenova, A. M.; Kuznetsova, T. A.; Denisenko, V. A.; Gorshkova, I. A.; Elyakov, G. B. *Khim. Prir. Soedin.* **1990**, *6*, 762–765.
5. El Sayed, K. A.; Hamann, M. T.; Waddling, C. A.; Jensen, C.; Lee, S. K.; Dunstan, C. A.; Pezzuto, J. M. *J. Org. Chem.* **1998**, *63*, 7449–7455.
6. Satyanarayana, S.; Satyavati, D. *Indian Drugs* **2000**, *37*, 102–104.
7. Zheng, Q.; Su, J.; Zeng, L. *Zhongshan Daxue Xuebao, Ziran Kexueban* **1990**, *29*, 54–58 (CAN 114:23704).
8. Zheng, Q.; Su, J.; Zeng, L. *Zhongshan Daxue Xuebao, Ziran Kexueban* **1990**, *29*, 106–110 (CAN 114:163848).
9. Zheng, Q.; Su, J.; Zeng, L. *Chin. Sci. Bull.* **1992**, *37*, 86–87 (CAN 117:8233).
10. Zheng, Q.; Su, J.; Zeng, L. *Zhongshan Daxue Xuebao, Ziran Kexueban* **1992**, *31*, 119–122 (CAN 118:59479).
11. Zheng, Q.; Su, J.; Zeng, L. *Zhongshan Daxue Xuebao, Ziran Kexueban* **1992**, *31*, 126–129 (CAN 119:72869).
12. Czarkie, D.; Carmely, S.; Groweiss, A.; Kashman, Y. *Tetrahedron* **1985**, *41*, 1049–1056.
13. Kobayashi, M. *J. Chem. Res., Synop.* **1991**, *11*, 310–311.
14. Katsuyama, I.; Fahmy, H.; Khalifa, S. I.; Kilada, R. W.; Zjawiony, J. K. *Book of Abstract*, 217th ACS National Meeting, Anaheim, California, March 21–25, 1999.
15. Torok, D. S.; Ziffer, H.; Meshnick, S. R.; Pan, X.; Ager, A. *J. Med. Chem.* **1995**, *38*, 5045–5050.
16. El Sayed, K. A.; Hamann, M. T. *J. Nat. Prod.* **1996**, *59*, 687–689.
17. Greenland, G. J.; Bowden, B. F. *Aust. J. Chem.* **1994**, *47*, 2013–2021.
18. El Sayed, K. A.; Dunbar, D. C.; Goins, K. D.; Cordova, C. R.; Perry, T. L.; Wesson, K. J.; Sanders, S. C.; Janus, S. A.; Hamann, M. T. *J. Nat. Toxins* **1996**, *5*, 261–285.